

CONTROL AND OPTIMIZATION OF TURBOCHARGED SPARK IGNITED ENGINES

Lars Eriksson* Simon Frei* Christopher Onder*
Lino Guzzella*

* *ETH Zurich, Switzerland*

Abstract:

The subject of this study is the trade-off between fuel economy and transient performance in turbocharged engines. It quantifies the losses and gains of different engine control strategies. Two extreme strategies are analyzed, one for optimal fuel economy and the other for fast transient response. Models for the components that influence the fuel economy are developed and described. An optimization problem for best fuel economy is solved analytically and a fuel-optimal controller is implemented based on that result. This controller is compared to one which is optimized for fast transient response with respect to the gains in fuel economy and losses in transient response. Simulations of a highly boosted engine show that a fuel-optimal controller can improve the fuel economy of a vehicle operated at cruising speed by 1-3% and at highway speed by 4%, and that the highest achievable improvement is above 10%. The losses in transient response are around 0.4 s for cruising conditions. Furthermore, measurements on a low-boosted engine on a test bench are used to show that the fuel-optimal controller reduces fuel consumption by 1.9% at highway conditions.

Keywords: Engine control, turbocharging, response time, fuel consumption.

1. INTRODUCTION

Customer demands for vehicles with a low fuel consumption are among the main driving forces for the technical development of engines and vehicles. However, customers do not sacrifice driveability for a reduced fuel consumption. Downsizing and supercharging concepts are one promising way of reducing the fuel consumption while delivering the same rated power, as presented in detail in Guzzella *et al.* (2000) and Soltic (2000). In turbocharged engines the demands for best fuel economy and good driveability are conflicting goals for the control system design. Current industry practice is to optimize the system for driveability, i.e., for the fastest possible transient response, with a sacrifice in efficiency. The aim here is to quantify the gain in fuel economy and the loss in response time if a control strategy for best fuel economy is used instead.

2. SYSTEM OVERVIEW AND TC MATCHING

In a turbocharged engine, the exhaust enthalpy is used to compress the air in the intake manifold and thus to achieve an increase in mass flow through the engine \dot{m}_a . The engine investigated in this paper is highly boosted, i.e., it runs with a maximum intake manifold pressure of $p_{im,max} = 2$ bar. An overview of the engine is given in Figure 1. The system has two control inputs: the throttle signal u_{th} which affects the intake manifold pressure p_{im} , and the waste gate signal u_{wg} which affects the exhaust back pressure p_{em} and the boost pressure p_c .

When the system has to reach a certain state, e.g., when the torque Tq_e and engine speed N are fixed, one degree of freedom remains. This degree of freedom can either be used to keep the compressor

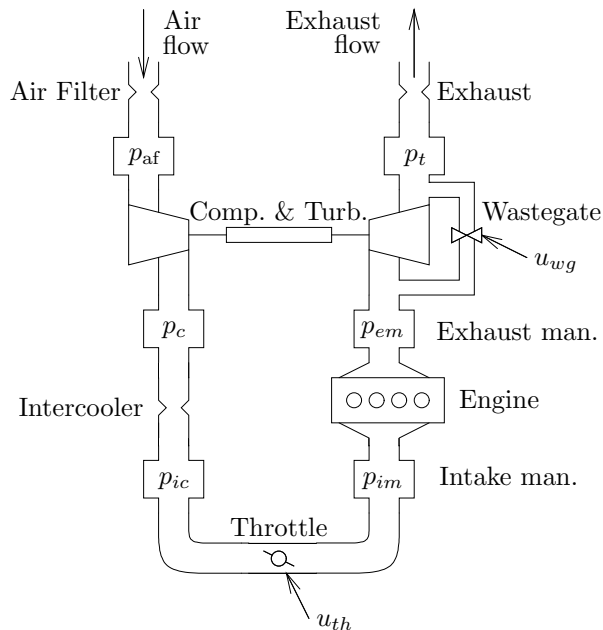


Fig. 1. Overview of the engine. The model consists of six receivers for each of which the pressure variable is shown.

speed at its highest possible level, which provides a fast transient response, or to lower the back pressure, which ensures good fuel economy. This leads to two different control strategies that will be described in section 6.

Matching up a compressor, a turbine, and an engine is a complex task that involves several steps. The following procedure is a simplification, but it illustrates the key steps: 1) Determine engine displacement and maximum engine power, which results in data on the boost level and on the maximum air mass flow. 2) Determine the compressors that fulfill those requirements and that reach the desired boost pressure without surging at the lowest flows possible. 3) Determine the turbines that drive the compressors as closely to the surge line as possible without generating too high a back pressure. Based on this procedure, simulations and experiments are done to find the compressor and the turbine that best match a set of given performance criteria.

Three-way catalytic converters are typically used to reduce emissions by requiring the engine to operate at stoichiometric conditions, i.e., $\lambda = 1$. We thus focus our investigation on engines operating at $\lambda = 1$, thus ignoring the problem that current turbine materials cannot withstand temperatures above 1300 K. Current practice is to protect the turbine at high air mass flows by fuel enrichment, which significantly raises the levels of pollutants and the fuel consumption.

3. OPTIMAL FUEL ECONOMY: FORMULATION OF THE PROBLEM

The brake-specific fuel consumption BSFC is defined as the fuel mass flow \dot{m}_f^* divided by the generated power P

$$\text{BSFC} \triangleq \frac{\dot{m}_f^*}{P} = \frac{\dot{m}_f^*}{Tq 2\pi N}$$

where N is the engine speed in revolutions per second. One problem with the definition of BSFC is that there is a singularity at zero torque. Therefore it is advantageous to look at $\frac{1}{\text{BSFC}} = Tq 2\pi N / \dot{m}_f^*$ which then has to be maximized for best fuel efficiency. Optimizing the cruising scenario with constant speed for the best fuel economy is thus the same as maximizing Tq / \dot{m}_f^* .

For cruising we now also consider the maximization under limited resources, that is a desired fuel flow $\dot{m}_{f,des}^*$, which now becomes

$$\begin{aligned} \max \quad & Tq(u_{th}, u_{wg}, \dot{m}_f^*) \\ \text{subject to} \quad & \dot{m}_f^*(u_{th}, u_{wg}) = \dot{m}_{f,des}^* \end{aligned}$$

A constant fuel flow corresponds to a constant air flow, since we are restricting engine operation to stoichiometric conditions. This leads to the following formulation of the problem

$$\begin{aligned} \max \quad & Tq(u_{th}, u_{wg}, \dot{m}_a^*) \\ \text{subject to} \quad & \dot{m}_a^*(u_{th}, u_{wg}) = \dot{m}_{a,des}^* \end{aligned} \quad (1)$$

4. MODELING OF A TURBOCHARGED ENGINE

The structure incorporates a number of control volumes which are separated by flow restrictions (see Figure 1). As a detailed explanation of the complete model would exceed the scope of this paper, only the components necessary for studying the problem of fuel optimality are described in the following paragraphs.

The formulation of the fuel-optimal operation of turbocharged SI engines shows that models for engine torque and engine air-mass flow are necessary. Since the control inputs affect the intake and exhaust manifold pressures, the models must describe how these pressures influence the torque levels and the air flow.

4.1 Engine Air Mass Flow

The air mass flow to the engine is modeled using the volumetric efficiency η_{vol} which provides the data necessary to calculate the amount of fresh

gases in the displaced volume V_d . The air mass flow is

$$\dot{m}_a(N, p_{im}, T_{im}, p_{em}) = \eta_{vol} \frac{V_d N p_{im}}{2 R T_{im}} \quad (2)$$

with T_{im} representing the intake manifold temperature. Since the intercooler efficiently takes away the temperature increase produced by the compressor, T_{im} is assumed to be constant.

The volumetric efficiency η_{vol} depends on the valve overlap as well as on the intake and exhaust manifold pressures, see e.g., the model by Fox *et al.* (1993). Since the engine considered here is highly boosted, the valve overlap can be assumed to be very small, in order to avoid scavenging losses. Therefore the residual gas mass is considered to be a function of the exhaust manifold state and of the clearance volume only. In the ideal Otto cycle, with no valve overlap, the volumetric efficiency is given by

$$\eta_{vol} = C_{\eta_{vol}} \frac{r_c - \left(\frac{p_{em}}{p_{im}}\right)^{1/\gamma}}{r_c - 1} \quad (3)$$

where $C_{\eta_{vol}}$ is a constant, γ is the ratio of specific heats, and r_c is the compression ratio.

4.2 Engine Torque

The engine torque is modeled on the basis of the work produced, where net work W_n is determined from the gross indicated work W_{ig} , produced by the high-pressure part of the engine cycle, minus the sum of pumping and friction work $W_p + W_f$ during one cycle.

$$Tq = \frac{W_n}{4\pi} = \frac{W_{ig} - W_p - W_f}{4\pi} \quad (4)$$

The gross indicated work is

$$W_{ig} = m_f q_{HV} \eta_{ig}$$

where q_{HV} is the lower heating value of the fuel and m_f is the injected fuel mass per engine cycle. The gross indicated efficiency η_{ig} depends on the thermodynamic cycle and heat transfer. It is assumed to be independent of p_{im} and p_{em} . The pumping work is

$$W_p = V_d (p_{em} - p_{im})$$

and the friction work is

$$W_f = V_d \cdot \text{FMEP}(N, \dot{m}_f^*)$$

where the friction mean effective pressure FMEP depends mainly on the speed. The slight dependence on engine load is captured by the variable \dot{m}_f^* .

The FMEP model used here is based on the ETH model (Inhelder, 1996; Stöckli, 1989). With this parameterization, the friction model as well is independent of p_{im} and p_{em} .

4.3 Compressor and Turbine

The pressure ratios over the components are defined as the pressure after the device divided by the pressure before the device, which for the compressor and turbine pressure ratios may be expressed as follows:

$$\Pi_c \triangleq \frac{p_c}{p_{af}} > 1, \quad \Pi_t \triangleq \frac{p_t}{p_{em}} < 1$$

Compressor and turbine performance is usually available in terms of maps measured in a flow bench by the manufacturer. These maps show the interrelationships among speed, flow, pressure ratio, and efficiency. The mechanical efficiency of the turbocharger is usually included in the efficiency map for the turbine.

Steady-state operation is determined from the power balance of the turbine and the compressor.

$$P_t = P_c \quad (5)$$

The power consumed by the compressor is

$$P_c = \frac{\dot{m}_a c_{p,a} T_{bc} \left[\Pi_c^{\frac{\gamma-1}{\gamma}} - 1 \right]}{\eta_c} \quad (6)$$

where η_c is the compressor efficiency. The power delivered by the turbine is

$$P_t = \dot{m}_e c_{p,e} T_{bt} \left[1 - \Pi_t^{\frac{\gamma-1}{\gamma}} \right] \eta_t \quad (7)$$

where η_t is the turbine efficiency.

5. OPTIMAL FUEL ECONOMY: THE SOLUTION

With the models at hand we once again turn to the problem of fuel-optimal control introduced by eqn. (1). Studying the torque model under the constraints of constant speed and constant fuel mass flow and with the modeling assumptions, we see that the only term affected by the control inputs is the pumping work. Thus, maximizing (4) for constant fuel mass is identical to minimizing pumping work W_p . Dividing W_p by the constant V_d yields the following function to be minimized:

$$U(p_{em}, p_{im}) = p_{em} - p_{im}$$

In turbocharged engines it is possible to have a p_{im} that is higher than p_{em} , which means that the pumping actually produces energy. It is now of great interest to see if the controller can take advantage of this effect to increase the engine output torque and fuel economy. However, as will be shown below, this is not the case, allowing the following fuel optimality statement to be made:

The optimal controller for problem (1) always minimizes p_{im} and p_{em} if the air flow model (2), (3) and the following inequality hold

$$\left(\frac{p_{im}}{p_{em}}\right)^{\frac{\gamma-1}{\gamma}} < 7 \quad (8)$$

At first glance this statement contradicts common sense since the pumping losses seem to be lowered when p_{im} is increased. In the next section, first the statement and then inequality (8) will be justified.

5.1 Justification of fuel optimality statement

First the fuel mass flow constraint is studied. For a given air mass flow through the engine, eqs. (2) and (3) define the relation between the intake manifold and exhaust manifold pressures. By manipulating (2) and (3) the following function can be defined

$$f_e(p_{im}) \triangleq \frac{p_{em}}{p_{im}} = \left(r_c - \frac{\dot{m}^*}{a p_{im}}\right)^\gamma \quad (9)$$

where $a = \frac{C_{nvol} V_d N}{(r_c-1) 2 R T_{im}} > 0$. This function is always positive, and it is monotonously increasing with p_{im} , since

$$f'_e(p_{im}) = \underbrace{\left(r_c - \frac{\dot{m}^*}{a p_{im}}\right)^{\gamma-1}}_{>0} \frac{\gamma \dot{m}^*}{a p_{im}^2} > 0 \quad (10)$$

where $r_c - \frac{\dot{m}^*}{a p_{im}} > 0$ follows from (9) and from the fact that the air mass flow is positive. This relation says that p_{im} monotonously increases with p_{em} .

The function to be minimized, $U(p_{im}, p_{em})$, can be rewritten as a function with only one variable, $V(p_{im})$, using the definition of $f_e(p_{im})$

$$V(p_{im}) \triangleq p_{em} - p_{im} = p_{im}(f_e(p_{im}) - 1)$$

Its derivative is:

$$V'(p_{im}) = f'_e(p_{im}) p_{im} + f_e(p_{im}) - 1$$

Now we have to prove that $V'(p_{im}) > 0$ for all possible values of p_{im} . First of all, if $f_e(p_{im}) > 1$ then (10) shows that $V'(p_{im}) > 0$ (which is $p_{em} > p_{im}$ and approximately naturally aspirating mode of the supercharged engine). Thus the optimal strategy is to minimize p_{im} in this region.

The case that remains to be investigated is

$$f_e(p_{im}) < 1 \quad (11)$$

Inserting (10) into $V'(p_{im})$ and manipulating the resulting equation yields

$$\begin{aligned} V'(p_{im}) &= \left(r_c - \frac{\dot{m}^*}{a p_{im}}\right)^{\gamma-1} \frac{\gamma \dot{m}^*}{a p_{im}} + f_e(p_{im}) - 1 \\ &= f_e(p_{im})^{\frac{\gamma-1}{\gamma}} \gamma \left(r_c - f_e(p_{im})^{\frac{1}{\gamma}}\right) + f_e(p_{im}) - 1 \end{aligned}$$

Finally, (11) together with (8) can be used to show that since $\gamma > 1$ and $r_c \geq 8$ the derivative is positive.

$$\begin{aligned} V'(p_{im}) &= \underbrace{f_e(p_{im})^{\frac{\gamma-1}{\gamma}}}_{>\frac{1}{7}} \underbrace{\gamma}_{>1} \underbrace{\left(r_c - f_e(p_{im})^{\frac{1}{\gamma}}\right)}_{<1} + \underbrace{f_e(p_{im})}_{>0} - 1 \\ &\quad \underbrace{\hspace{10em}}_{>r_c-1} \\ &> \frac{1}{7} (r_c - 1) - 1 > 0 \end{aligned}$$

The fact that $r_c \geq 8$ is derived in Soltic (2000) where a database of production engines was investigated and the smallest compression ratio for a turbocharged engine was found to be 8. The fuel optimality statement is thus justified.

5.1.1. Justification of (8) Inequality (8) defines a bound on the pressure ratio over the engine for which the fuel optimal statement is valid. Evaluating the bound for $\gamma = 1.4$ yields $\frac{p_{im}}{p_{em}} < 910$. This is much higher than all attainable values of the pressure ratio. Currently the highest pressure ratios delivered by compressors start reaching values of 6, so there is a very large margin. However, this margin is not satisfactory since it relies upon current compressor limitations. We thus seek a theoretical upper limit on the pressure ratio. Inserting (6) and (7) into the power balance (5) yields

$$\frac{\Pi_c^{\frac{\gamma-1}{\gamma}} - 1}{1 - \Pi_t^{\frac{\gamma-1}{\gamma}}} = \underbrace{\frac{\dot{m}_e c_{p,e} T_{bt}}{\dot{m}_a c_{p,a} T_{bc}} \eta_c \eta_t}_A$$

Multiplying both sides with $\Pi_t^{\frac{\gamma-1}{\gamma}} (1 - \Pi_t^{\frac{\gamma-1}{\gamma}})$ and solving for the following

$$\Pi_t^{\frac{\gamma-1}{\gamma}} \Pi_c^{\frac{\gamma-1}{\gamma}} = A \Pi_t^{\frac{\gamma-1}{\gamma}} \left[1 - \Pi_t^{\frac{\gamma-1}{\gamma}}\right] + \Pi_t^{\frac{\gamma-1}{\gamma}}$$

eventually yields

$$(\Pi_t \Pi_c)^{\frac{\gamma-1}{\gamma}} \leq \frac{(A+1)^2}{4A}$$

In order to get an upper bound on A , we assume the maximum temperature of the turbine inlet to be 1300 K, which is at the limit of what the turbine material can tolerate, and the lower limit on the inlet conditions to be 273 K, with the following limits for the fluid properties, $c_{p,e} > 1.34$ [J/g K], $c_{p,a} > 1.00$ [J/g K], and $\frac{\dot{m}_e}{\dot{m}_a} = 1 + \frac{1}{(A/F)_s} < 1.07$. Inserting these numbers, together with the definitions of the pressures, and noting that all turbines and compressors have efficiencies lower than unity leads to the following limit,

$$A < 6.73|_{\eta_c=\eta_t=1} \Rightarrow \left(\frac{p_{im}}{p_{em}}\right)^{\frac{\gamma-1}{\gamma}} < 2.3$$

This limit of 2.3, based on the above assumed physics, is much lower than the value of 7 and therefore (8) holds in any realistic case.

6. CONTROL DESIGN

The fuel optimality statement says that it is always favorable to lower p_{im} and p_{em} as much as possible. The strategy indicated by this statement is to open the waste gate (or in the case of a variable nozzle turbine to open the nozzles) as much as possible. The controller to achieve this can be described as follows.

6.1 Layout 1: Fuel-optimal controller

Starting from low load the waste gate is fully open and the throttle is used to control the load. Only after the throttle is fully open the waste gate starts to close and controls the intake manifold pressures above ambient pressure.

6.2 Layout 2: Driveability-optimized controller

In current series production cars the time-optimal strategy is implemented. The goal of this strategy is to keep the turbocharger on the highest possible speed. This is due to the fact that the rotational dynamics of the turbocharger are the limiting factor for the time response. This is achieved by closing the waste gate as much as possible until an appropriate boost pressure after the compressor p_c is reached. This level lies above the maximum of p_{im} , since the intercooler and the open throttle act as flow restrictions. In this strategy the throttle is used for load control and the waste gate is only used to limit the boost pressure.

7. COMPARISON OF THE TWO CONTROLLER VERSIONS

7.1 Difference in fuel economy

Figure 2 shows the improvement in fuel economy that can be achieved when using the fuel-optimal controller. The gains are especially high for low loads and high engine speeds. But the most interesting points are those below 3500 rpm and 10 bar BMEP, as more than 60% of the operating time fall into that region. The improvement in fuel economy for cruising conditions, approximately 2000 rpm and 6 bar BMEP, is around 2%, whereas for highway driving with higher speeds and loads the improvement is around 4%.

7.1.1. Experimental validation Measurements have been performed on a mildly-boosted turbocharged SAAB 2.3 liter engine to validate the predicted gains in fuel economy. Since the engine only has low boosting, the gain in fuel economy will be lower than the gains shown in Figure 2. The

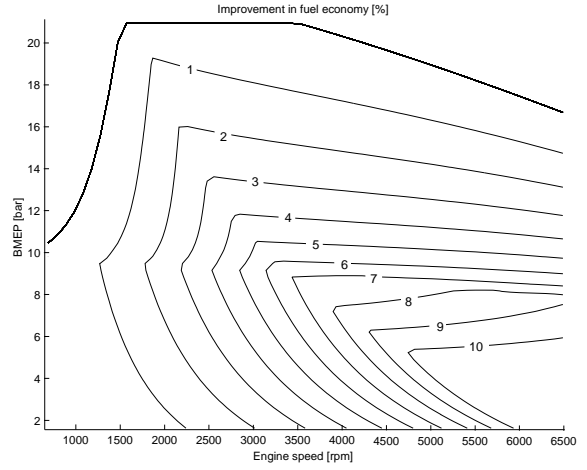


Fig. 2. Simulated improvement in brake-specific fuel consumption at steady state when using the fuel-optimal controller.

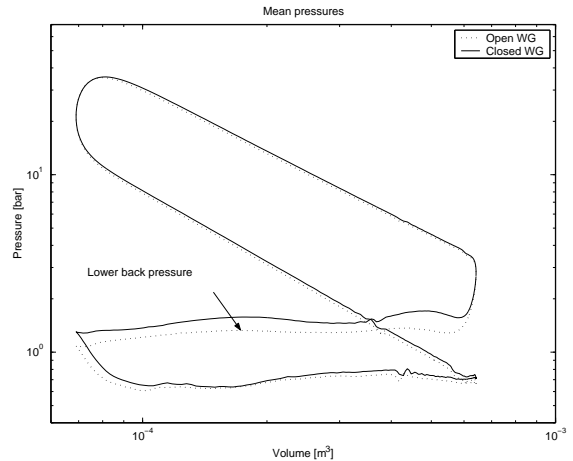


Fig. 3. Plot showing measured cylinder pressure averaged over 40 cycles for the two control strategies at the same air mass flow and engine speed. In the plot the decreased back pressure is clearly shown, which decreases the pumping losses.

conditions for the test are the same as for (1). Two measurements at the same engine speed and with the same air mass flow are made, one with the wastegate fully closed and one with it fully open. The speed, mass flow, and λ are controlled using three closed-loop controllers. The operating condition was an engine speed of 3200 rpm and a BMEP of 5.8 bar.

The cylinder pressures from the two measurements are plotted in Figure 3. Quite obviously, the exhaust back pressure is decreased when the wastegate is open. In the measurements, the torque increased from 103.55 to 105.51 Nm when the wastegate was opened, which reflects an efficiency increase of 1.9%.

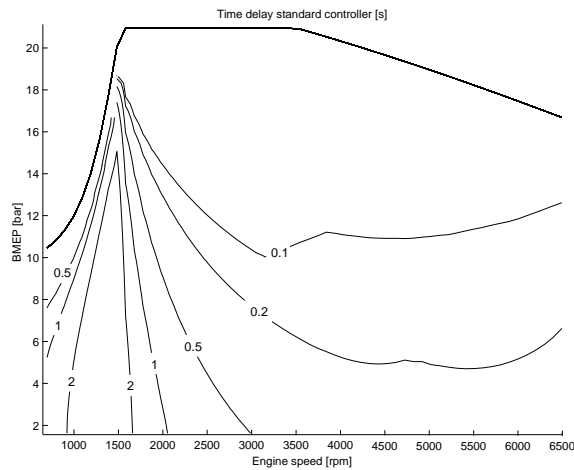


Fig. 4. Simulated time to reach 90% of torque after tip-in with a driveability-optimized controller

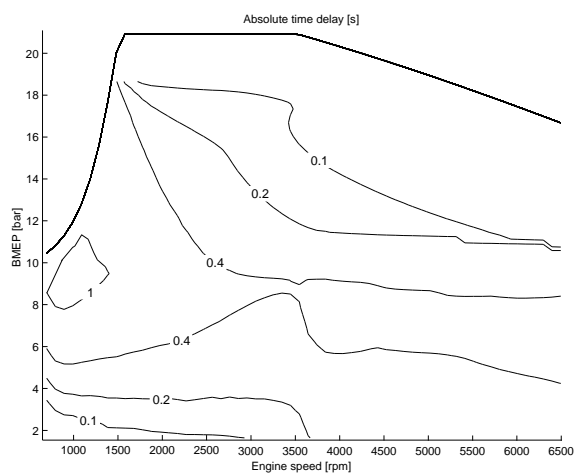


Fig. 5. Simulated difference in response time between the standard and fuel-optimal controller.

7.2 Difference in response time

In order to study the torque development and torque response times, a constant engine speed test case was used to isolate the results from gearbox and vehicle influences. The response time is measured as the time delay from tip-in to the instant when the torque reaches a value of 90% of the maximum that is achievable at that speed.

The response time for the standard controller is shown in Figure 4. The large delay around 1500 rpm is due to the low air mass flow and the high torque level achievable. Below this speed the maximum torque decreases and can therefore be attained faster.

The engine with the fuel-optimal controller has a longer response time since it starts with a lower speed of the turbocharger. Figure 5 shows the differences in response times between the fuel-optimal and standard controllers. The additional time delay is around one-half of a second for normal cruising conditions.

7.3 Discussion of the strategies

As turbocharged engines are known to suffer from an inherently bad dynamic behavior, the additional deterioration shown in Figure 5 might not be acceptable.

A solution to this problem is to detect the driver's intention. If an upcoming acceleration could be detected one-half of second in advance, 95% of the engine states could be handled (see Figure 5). Another solution would be to connect the choice of the control strategy to an "Eco Button", with which the driver could choose between the good fuel economy and the fast transient response.

8. SUMMARY AND CONCLUSIONS

The question of how a fuel-optimal controller for a turbocharged spark-ignited engine has to be designed has been investigated. An analytical investigation showed that under the mentioned simplifications, it is always advantageous to keep the pressures before and after the engine as low as possible. This leads directly to the proposed fuel-optimal controller that opens the waste gate as much as possible without reducing the desired air mass flow.

This new strategy was compared with a standard controller which tries to keep the speed of the turbo charger as high as possible. Simulations show that the fuel-optimal controller can improve the fuel economy at cruising speed by around 1-3%, at highway speed by 4%, and that the highest achievable improvement is above 10%. This improvement comes at the expense of longer response times. In the operating region where the fuel economy was compared, the response time for the torque was increased by up to a second.

REFERENCES

- Fox, J., W. Cheng and J. Heywood (1993). A Model for Predicting Residual Gas Fraction in Spark-Ignition Engines. *SAE Technical Paper 931025*.
- Guzzella, L., U. Wenger and R. Martin (2000). IC-engine downsizing and pressure-wave supercharging for fuel economy. *SAE Technical Paper 2000-01-1019*.
- Inhelder, J. (1996). Verbrauchs- und Schadstoffoptimiertes Ottomotor-Aufladekonzept. Dissertation no 11948, ETH Zürich
- Soltic, Patrik (2000). Part-Load Optimized SI Engine Systems. Dissertation no 13942, ETH Zürich
- Stöckli, M. (1989). Reibleistung von 4-Takt Verbrennungsmotoren. Internal report of the Laboratory of Internal Combustion Engines, ETH Zürich